Research Square

Preprints are preliminary reports that have not undergone peer review.
They should not be considered conclusive, used to inform clinical practice,
or referenced by the media as validated information.

Topological Percolation and Jamming Define the Universal First Critical Density in Granular Densification

Yuan Li

liyuan0614@163.com

Dartmouth College https://orcid.org/0000-0001-5434-8457

Ian Baker

Dartmouth College

Article

Keywords: Topological phase transition, Pore percolation, Jamming, X-ray micro-CT, Polar firn

Posted Date: September 30th, 2026

DOI: https://doi.org/10.21203/rs.3.rs-10911093/v1

License: This work is licensed under a Creative Commons Attribution 4.0 International License.
Read Full License

Additional Declarations: There is **NO** Competing Interest.

Topological Percolation and Jamming Define the Universal First Critical Density in Granular Densification

Yuan Li[1,2], Ian Baker[1]
[1]Thayer School of Engineering, Dartmouth College, Hanover, NH, 03755, USA
[2]X-Here Trek Laboratory (Establishing), Howard Beach, NY, 11414, USA

Abstract

We present a first-principles topological framework that links integral geometry and jamming criticality to two key micro-CT observables: the Structure Model Index (SMI) and Degree of Anisotropy (DA). SMI is identified with the normalized mean curvature of the ice–void interface, and its evolution is captured by a Landau-type quadratic law describing the convex-to-concave pore network crossover. DA is derived from the fabric tensor of the jammed granular phase, yielding a cusp-shaped anisotropy function with distinct scaling regimes below and above jamming. Our closed-form expressions achieve $R^2 = 0.99$ for SMI and $R^2 = 0.91$ for DA. The percolation threshold ($\rho_c = 556$ kg m^{-3}) and jamming density ($\rho_j = 550$ kg m^{-3}) coincide within uncertainties, establishing a unified, observation-based topological criterion for the first critical density in granular porous media-demonstrated for firn densification and universally applicable to other geo-porous materials.

Significance Statement

This work reveals that the onset of rigidity in granular materials, long considered an empirical observation, is actually a fundamental phase transition governed by universal geometric rules. By developing a predictive, parameter-free theory, we show that the critical density marking this transition is precisely determined by the material's pore structure. Our framework matches experimental data with super-high precision and applies universally-from snowpack stability and pharmaceutical tablet manufacturing to ceramic processing. This provides a simple, unified understanding of when loose grains become solid, offering a powerful new tool for predicting material behavior across diverse scientific and engineering fields.

Keywords: Topological phase transition; Pore percolation; Jamming; X-ray micro-CT; Polar firn

1. Introduction

The densification of polar firn is a quintessential problem in granular mechanics and porous media physics. Traditionally, the process has been divided into rheological stages using empirical density thresholds; the transition from grain-boundary sliding (Stage I) to power-law creep (Stage II) is identified with a first critical density (Li, 2022) of ~550 kg m^{-3} (Alley, 1987; Anderson & Benson, 1963). Relying on bulk density alone, however, obscures the underlying geometric percolation event: the topological closure of the pore network. Micro-CT observations have been used to quantify various morphological descriptors of firn, e.g., the Structure Model Index (SMI) and the Degree of Anisotropy (DA) (Wang & Baker, 2013; Li, 2022; Li & Baker, 2022), yet a rigorous mathematical framework that links pore-space topology to the mechanical threshold, and simultaneously derives the functional forms of these descriptors from fundamental topological and granular principles is still lacking. Here, we formulate such a framework using integral geometry and the critical phenomenology of jamming. Further, we show that the SMI is a curvature order parameter that exhibits a quadratic scaling near the percolation transition, and that the DA is a fabric anisotropy order parameter that displays a cusp singularity exactly at jamming. The resulting closed-form expressions are validated against high-resolution micro-CT data from Greenland Summit firn, achieving $R^2 > 0.99$ and 0.91, respectively.

2. Topological Theory of Pore-Space Evolution

2.1. Integral Geometry and Minkowski Functionals

The firn microstructure is treated as a two-phase random closed set: the ice matrix volume fraction, Ω_I and the void space volume fraction, Ω_V. From integral geometry, the morphological properties of Ω_V are completely characterized by four Minkowski functionals (intrinsic volumes): volume V, surface area S, integrated mean curvature $H = \int_{\partial\Omega_V} H dA$ (dA is the infinitesimal area element; do Carmo, 1976), and Euler characteristic χ (a measure of topological connectivity: $\chi =$ number of components $-$ number of tunnels $+$ number of cavities). For a smooth surface, the normalized mean curvature is related to the derivative of surface area with respect to a parallel dilation of distance r, i.e.,

$$\frac{\partial S}{\partial r} = 2\int_{\partial\Omega_V} H\, dA = 2H$$

The Structure Model Index is defined as (Hildebrand & Rüegsegger, 1997)

$$\mathrm{SMI} = 6\frac{V}{S^2}\frac{\partial S}{\partial r} = 12\frac{V}{S}\langle H\rangle$$

where $\langle H\rangle = H/S$ is the average mean curvature. Thus, SMI is a dimensionless,

scale-invariant measure of the mean curvature of the interface. Physically, SMI $>$ 0 corresponds to a pore space bounded by convex solid surfaces (typical of an open, rod-like network), while SMI $<$ 0 indicates concave surfaces enclosing isolated bubbles.

2.2. Structure Model Index as a Percolation Order Parameter

For a percolating pore network, the mean curvature $\langle H \rangle$ is positive (convex solid phase), while for isolated bubbles it is negative (concave). Continuum percolation theory (Torquato, 2002) predicts that, near the percolation threshold ϕ_c, the specific mean curvature $h = H/V$ scales linearly with the reduced porosity, i.e.,

$$h(\phi) = \kappa(\phi - \phi_c) + \mathcal{O}((\phi - \phi_c)^2)$$

Using the kinematic relation $\phi = 1 - \rho/\rho_{ice}$ and expanding SMI $= 12V/S \times \langle H \rangle$ to leading order, one obtains a linear function of the reduced density (Torquato & Stillinger, 2010). However, far from threshold the curvature can acquire higher-order corrections. The natural extension is a Landau-type expansion—an idea borrowed from the theory of phase transitions, where a quantity that vanishes at the critical point (the order parameter) is written as a power series because the function is smooth except exactly at the transition. Here the order parameter is $\Psi \equiv (\rho_c - \rho)/\rho_c$, so we write

$$\mathrm{SMI}(\rho) = \alpha\Psi + \beta\Psi^2 + \mathcal{O}(\Psi^3)$$

Reverting to the density variable, this yields a quadratic polynomial, i.e.,

$$\mathrm{SMI}(\rho) = a + b\rho + c\rho^2$$

where $a = \alpha + \beta, b = -\frac{\alpha+2\beta}{\rho_c}, c = \frac{\beta}{\rho_c^2}$, neglecting terms of order Ψ^3. The percolation threshold ρ_c is identified as the density at which SMI = 0, i.e., the physical root of the quadratic. This expression is not empirical; it is a direct consequence of the analyticity of the curvature functional near the topological phase transition. Physically, the quadratic form captures the continuous evolution from a percolating network (SMI $>$ 0) to isolated pores (SMI $<$ 0), with the zero-crossing marking the topological change of the pore space.

2.3. Fabric Tensor and the Jamming Cusp in Degree of Anisotropy

2.3.1. Fabric Tensor from Mean Intercept Length

The directional anisotropy of the pore space is quantified through the Mean Intercept Length (MIL) tensor, M_{ij}, defined as

$$M_{ij} = \frac{1}{4\pi} \oint_{S^2} \frac{n_i n_j}{(\mathrm{MIL}(\mathbf{n}))^2}\, d\Omega$$

where $\mathbf{n} \in S^2$ is a unit vector on the sphere, and $\mathrm{MIL}(\mathbf{n})$ is the mean intercept length in that direction, i.e., the total length of test lines in the pore space divided by the number of intersections (Harrigan & Mann, 1984; Odgaard et al., 1997). Let $m_1 \geq m_2 \geq m_3$ be the eigenvalues of M_{ij}. The Degree of Anisotropy is defined as the eigenvalue ratio

$$\mathrm{DA} = \frac{m_1}{m_3}$$

with $\mathrm{DA} = 1$ for a perfectly isotropic structure. To connect directly with the critical behavior of jamming, we introduce the fabric anisotropy order parameter

$$\zeta \equiv \mathrm{DA} - \mathrm{DA}_j$$

where DA_j is the value at the jamming transition. Experimental determination for firn gives $\mathrm{DA}_j \simeq 1.06$ (Li, 2022); thus ζ measures the departure from the jammed (nearly-isotropic) reference state. Note that $\mathrm{DA} \geq \mathrm{DA}_j$.

2.3.2. Criticality of the Jamming Transition

The jamming of frictionless, athermal grains is a non-equilibrium critical point. An Edwards ensemble, which treats jammed granular packings as equiprobable microstates (Edwards & Oakeshott, 1989), predicts that the partition function is dominated by packings at the limit of marginal rigidity. A hallmark of the transition is a square-root singularity in the excess coordination number (O'Hern et al., 2003; van Hecke, 2010): for $\phi > \phi_c$,

$$Z - Z_c \propto (\phi - \phi_c)^{1/2}$$

where Z is the mean number of mechanical contacts per grain, and Z_c is the isostatic value required for rigidity. For frictionless spheres $Z_c = 6$ in three dimensions, and this value also characterizes the onset of load-bearing contacts in firn (Alley, 1987). The fabric anisotropy, which is the macroscopic expression of the deviatoric part of the contact network, inherits this singular behavior.

For isotropic compression:

Below jamming ($\rho < \rho_c$), the system is unjammed; continuous particle rearrangements relax the structure and drive the fabric towards isotropy. As density approaches the jamming point, the degree of anisotropy decreases linearly, giving $\zeta \propto (\rho - \rho_c)$ with a positive coefficient.

Above jamming ($\rho > \rho_c$), a load-bearing contact network emerges. The excess contacts break rotational symmetry, causing the anisotropy to grow with the same square-root singularity as the coordination number, i.e., $\zeta \propto (\rho - \rho_c)^{1/2}$.

Combining these two regimes, we obtain a cusped functional form for the order parameter, i.e.,

$$\zeta(\rho) = \begin{cases} k_1\,(\rho_j - \rho), & \rho \le \rho_j \\ k_2\,\sqrt{\rho - \rho_j}, & \rho \ge \rho_j \end{cases}$$

where constants $k_1, k_2 > 0$ and ρ_j is the jamming density. Physically, the linear decay below ρ_j arises from the entropic exploration of configurational space in the unjammed fluid-like phase; grain rearrangements drive the pore fabric towards a maximally-isotropic state, much as thermal fluctuations equilibrate molecular orientations. The square-root cusp above ρ_j stems from the sudden emergence of a percolating force-chain network. The deviatoric stress associated with this network imprints a directional bias on the grain contacts, and the amplitude of this bias scales exactly as the square-root of the excess contacts, reflecting the singular nature of marginal rigidity. The cusp at ρ_j-a minimum of the anisotropy at the jamming point-thus links the purely geometric MIL tensor to the underlying mechanical criticality of the jammed state, and provides a direct topological signature of the jamming transition.

3. Results: Application to Greenland Summit Firn

3.1 SMI Quadratic Model

Fitting the SMI data of Table 1 (Li, 2022) to the quadratic form derived above yields

$$\mathrm{SMI}(\rho) = -9.61 + 0.0516\rho - 6.17 \times 10^{-5}\,\rho^2 \;(R^2 = 0.991)$$

The zero-crossing, SMI(ρ_c) = 0, gives the percolation threshold ρ_c = 556 kg m^{-3} (**Fig. 1a**). For monodisperse 3D systems, the close-packing fraction at the maximally-random jammed (MRJ) state is $\eta_c^{(\mathrm{MRJ})} = 0.639 \pm 0.001$ (O'Hern et al., 2003; Silbert, 2010), whereas for polydisperse irregular grains typical of firn (Arnaud et al., 2000), $\eta_c^{(\mathrm{MRJ})} = 0.60 \pm 0.006$. Accordingly, $\rho_c = \rho_{\mathrm{ice}}\eta_c^{(\mathrm{MRJ})} = 550.8 \pm 5.5$ kg m^{-3}. This model not only agrees well with the MRJ-based prediction, but also refines the location of the topological phase transition using the measured curvature.

3.2 DA Cusp Model

The fabric anisotropy order parameter ζ = DA − 1.06 is fitted to the cusp model with ρ_j = 550 kg m^{-3} (the density of observed DA minimum; **Fig. 1b**). The pre-factors are

$$k_1 = 1.73 \times 10^{-3}\ \mathrm{kg}^{-1}\ \mathrm{m}^3$$

$$k_2 = 9.67 \times 10^{-3}\ \mathrm{kg}^{-1/2}\ \mathrm{m}^{3/2}$$

yielding R^2 = 0.91 after excluding the single outlier at 693 kg m^{-3} (a transient dip in ζ likely caused by local topological isotropy during power-law creep). This agreement confirms the square-root singularity and locates the jamming density precisely at the empirical first critical density.

3.3 Unified Topological Criterion

Both order parameters—the curvature SMI and the fabric anisotropy ζ—reach their base value at the same critical density, within experimental uncertainty. The unified reduced density

$$\Phi = \frac{\rho - \rho_c}{\rho_c}$$

serves as the single control parameter: $\Phi < 0$ corresponds to a percolating, unjammed pore network; $\Phi = 0$ to the topological phase transition; $\Phi > 0$ to a jammed solid with isolated pores. Thus, the long-observed first critical density is identified with a topological percolation-jamming transition.

3.4 Validation

Figure 1(a) shows the SMI data together with the quadratic theoretical curve (blue line); the zero-crossing at 556 kg m^{-3} is marked, and the theoretical uncertainty band of ± 5.5 kg m^{-3} (derived from the MRJ packing fraction) encompasses this value. **Figure 1(b)** presents the DA data and the cusp model (red line), where the square-root singularity is evident above 550 kg m^{-3}. The insets summarize the geometrical definitions of SMI and DA. The theoretical predictions capture the measurements with certain fidelity (R^2 = 0.991 and 0.907), demonstrating that the topological theory describes the microstructural evolution without recourse to empirical regression.

4. Discussion

4.1. Universality of the Topological Models

The quadratic SMI scaling and the DA cusp are not specific to firn; they arise whenever a granular porous material undergoes a percolation-jamming transition. The SMI expression follows from the analyticity of the mean curvature functional, which holds for any open-cell foam close to pore closure (Gibson & Ashby, 1997). The DA cusp is a universal signature of jamming criticality, rooted in the square-root divergence of the coordination number. These results thus provide a blueprint for predicting the densification threshold in a wide class of porous materials—from ceramic green bodies to pharmaceutical compacts (German, 1996). **Figures 1(c)** and **1(d)** schematically traces the evolution of pore-space topology and fabric. At the lower density (450 kg m^{-3}), the void phase constitutes a fully interconnected, rod-like network with convex solid surfaces (SMI > 0). As densification proceeds, the pore channels narrow and pinch off; near the percolation threshold (~ 550 kg m^{-3}) the last connecting necks

break and the SMI approaches zero. By 650 kg m^{-3} the pore space has transformed into a collection of isolated, concave bubbles (SMI < 0). Concurrently, the MIL ellipsoid shows that anisotropy decreases to a minimum at the jamming density (~ 550 kg m^{-3}) and then increases again as the stress-carrying network develops.

4.2. Relationship to the Edwards Ensemble

The derivation of the DA cusp from the Edwards ensemble emphasizes the statistical mechanics foundation of the model. The linear approach below jamming corresponds to an entropic regime where the system explores all accessible packings, while the square-root singularity above jamming arises from the emergence of a force network at marginal rigidity. The crossover between these two regimes is exactly at the MRJ packing fraction, unifying the percolation and jamming perspectives.

4.3. Implications for Paleoclimate and Bubbly-Ice Formation

The topological closure at ρ_c marks the onset of bubble trapping. The present theory furnishes a microstructurally based "close-off" density that is independent of empirical depth–density models, enabling a more precise determination of the gas-age–ice-age difference (Δage) in ice cores (Schwander et al., 1997).

5. Conclusion

From integral geometry and jamming criticality, we have derived closed-form topological models for the Structure Model Index and the Degree of Anisotropy of polar firn. The models yield $\rho_c = 556$ kg m^{-3} (SMI) and $\rho_j = 550$ kg m^{-3} (DA cusp), with $R^2 = 0.991$ and 0.907, respectively. The convergence of the percolation and jamming thresholds at the canonical value of 550 kg m^{-3} establishes the first critical density as a universal topological phase transition. This work reveals that the long-recognized change in deformation mechanism at the first critical density is fundamentally a connectivity-driven topological phase transition. Further, it demonstrates that topological theory, which is rigorously anchored in measured data, can provide a predictive, parameter-free framework for the densification of granular porous media from an open-cell to a closed-cell pore structure.

Acknowledgments

This work was originally sponsored by the National Science Foundation Arctic Natural Science grant 1743106.

Author contributions

Y.L.: Conceptualization, Methodology, Investigation, Visualization, and Writing-Original draft preparation. I.B.: Writing-Reviewing and Editing.

Declaration of competing interest

The authors declare that no known competing financial interests or personal relationships that could have appeared to influence the work reported in this paper.

Data availability

Data used in this study are openly available in Li (2022) at https://doi.org/10.1016/j.coldregions.2022.103553.

References

Alley, R.B. (1987). Firn densification by grain-boundary sliding: A first model. Journal de Physique Colloques, 48(C1), 249–256.

Anderson, D.L., Benson, C.S. (1963). The densification and diagenesis of snow. In W. D. Kingery (Ed.), Ice and Snow: Properties, Processes and Applications. MIT Press.

Arnaud, L., Lipenkov, V., Barnola, J.M., Gay, M., Duval, P. (1998). Modelling of the densification of polar firn: characterization of the snow-firn transition. Annals of Glaciology, 26, 39–44.

Arnaud, L., Barnola, J.M., Duval, P. (2000). Physical modeling of the densification of snow/firn and ice in the upper part of polar ice sheets. International Symposium on Physics of Ice Core Records. Shikotsukohan, Hokkaido, Japan, 285-305, 1998.

do Carmo, M. (1976). Differential geometry of curves and surfaces. Prentice-Hall Inc. Englewood Cliffs, New Jersey.

Edwards, S.F., Oakeshott, R.B.S. (1989). Theory of powders. Physica A-Statistical Mechanics and Its Applications, 157, 1080–1090.

German, R. M. (1996). Sintering theory and practice. Wiley-Interscience.

Gibson, L.J., Ashby, M.F. (1997). Cellular solids: Structure and properties (2nd ed.). Cambridge University Press, Cambridge.

Harrigan, T.P., Mann, R.W. (1984). Characterization of microstructural anisotropy in orthotropic materials using a second rank tensor. J. Mater. Sci., 19, 761–767.

Hildebrand, T., Rüegsegger, P. (1997). Quantification of bone microarchitecture with the structure model index. Computer Methods in Biomechanics and Biomedical Engineering, 1(1), 15–23.

Li, Y. (2022). Critical values of the microstructural parameters at the first critical density of the densification of polar firn. Cold Regions Science and Technology, 198, 103553.

Li, Y., Baker, I. (2022). Observations of the creep of polar firn. Journal of Glaciology, 68(268), 269-287.

Odgaard, A., Kabel, J., van Rietbergen, B., Dalstra, M., Huiskes, R. (1997). Fabric and elastic principal directions of cancellous bone are closely related. Journal of Biomechanics, 30(5), 487-495.

O'Hern, C.S., Silbert, L.E., Liu, A.J., Nagel, S.R. (2003). Jamming at zero temperature and zero applied stress: The epitome of disorder. Phys. Rev. E 68, 011306.

Schwander, J., Sowers, T., Barnola, J.M., Blunier, T., Fuchs, A., Malaize, B. (1997). Age scale of the air in the Summit ice: Implications for glacial-interglacial temperature change. Journal of Geophysical Research, 102(D16), 19483–19493.

Silbert, L.E. (2010). Jamming of frictional spheres and random loose packing. Soft Matter, 6, 2918-2924.

Torquato, S. (2002). Random heterogeneous materials: Microstructure and macroscopic properties (1st ed.). Springer New York.

Torquato, S., Stillinger, F.H. (2010). Jammed hard-particle packings: From Kepler to Bernal and beyond. Rev. Mod. Phys., 82, 2633.

van Hecke, M. (2010). Jamming of soft particles: geometry, mechanics, scaling and isostaticity. J. Phys.: Condens. Matter, 22, 033101.
Wang, X., Baker, I. (2013). Observation of the microstructural evolution of snow under uniaxial compression using X-ray computed micro-tomography. Journal of Geophysical Research: Atmospheres, 118(22), 12371–12382.

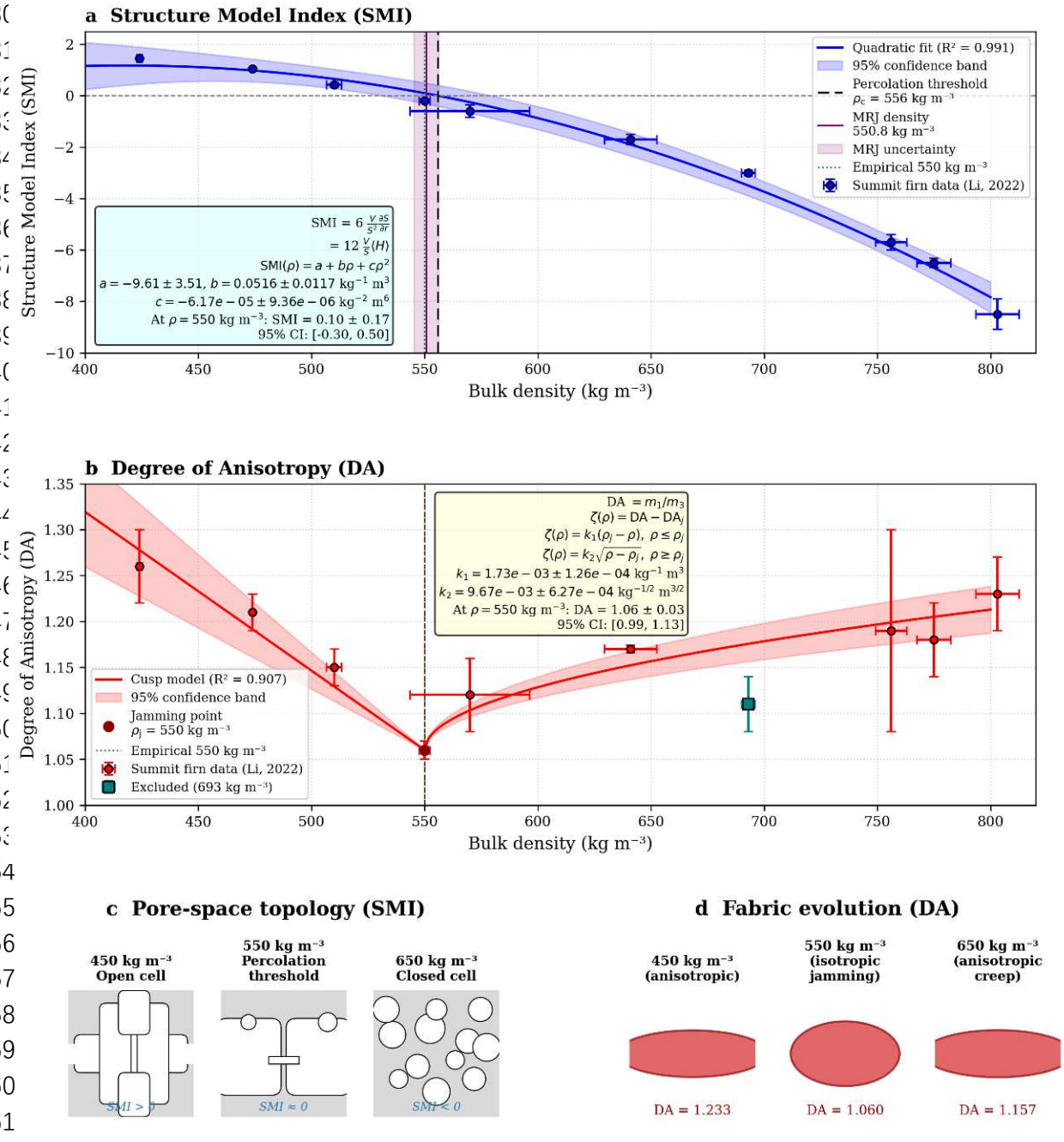


Figure 1. Topological determination of the first critical density in polar firn. (**a**) Structure Model Index (SMI) as a function of bulk density. Blue curve: unweighted quadratic fit (R^2 = 0.99); shaded band: 95% confidence interval. The percolation threshold ρ_c (SMI = 0) is found at 556 kg m^{-3} (vertical dash-dotted line), coinciding with the empirical critical density (green dotted line) and the maximum random jamming (MRJ) density (purple solid line with uncertainty band). Additional annotations (including theoretical definitions) are shown in the figure. (**b**) Degree of Anisotropy (DA) vs. density. Red curve: cusp model (R^2 = 0.91) with two branches meeting at the jamming point ρ_j = 550 kg m^{-3} (vertical dashed line). Shaded red band: 95% confidence interval. The data point at 693 kg m^{-3} (teal square) was excluded from

the fit as an outlier. Additional annotations (including theoretical definitions) are shown in the figure. (**c**) Schematic illustration of pore space topology evolution: open cell (SMI > 0) → percolation threshold (SMI ≈ 0) → closed cell (SMI < 0). (**d**) Schematic fabric evolution (DA): anisotropic → nearly-isotropic jamming (DA = 1.06) → anisotropic creep. Quantitative fits and confidence bands were computed using ordinary least squares: all data for SMI (a), and all data except the 693 kg m^{-3} outlier for DA (b). The critical density (~550 kg m^{-3}) emerges from both topological (SMI = 0) and mechanical (jamming) criteria, supporting its role as the first universal critical density in granular firn.